

# Characterization of Pt- and PtRu-Solid Polymer Membrane Electrodes for Methanol Electro-Oxidation Reaction in Direct Methanol Fuel Cell

Tanakorn Ratana,<sup>a\*</sup> Pongsaton Amornpitoksuk<sup>b</sup> and Waret Veerasai<sup>a</sup>

<sup>a</sup> Department of Chemistry, Faculty of Science, Mahidol University, Bangkok, 10400, Thailand.

<sup>b</sup> Department of Chemistry, Faculty of Science, Prince of Songkla University, Songkla, 90100 Thailand.

\* Corresponding author, E-mail: g4336103@yahoo.com

Received 22 Aug 2005

Accepted 9 Mar 2006

**ABSTRACT:** Nano-sized of Pt and PtRu particles on solid polymer electrode (SPE) membrane were prepared by the modified Takenaka-Torika (T-T) method. The morphological characteristics and catalyst compositions were also studied on the Pt- and PtRu-SPEs. The electrodes were characterized using electrochemical measurements, scanning electron microscope with electron dispersive microscope (SEM-EDX) and X-ray diffraction analysis. The well-dispersed Pt and PtRu alloy nanoparticles with crystallite size of 12-6 nm were obtained in the preparation. The differences in morphology of the nano-, micro-structure and composition of these catalysts effected the electro-catalytic activity of methanol electro-oxidation reaction. The electrochemical result showed that the mole ratio between Ru and Pt at 0.10 was the best condition for the methanol electro-oxidation reaction in partial cell study.

**KEYWORDS:** Takenaka-Torikai method, methanol electro-oxidation, SPE, XRD, DMFC.

## INTRODUCTION

Direct methanol fuel cell (DMFC) is considered as an alternative source of energy supply for modern equipment such as a portable power source and electrical supply in vehicles. As such, it is an interesting research area to improve the efficiency of fuel cell technology<sup>1-3</sup>. DMFC is an attractive choice because it removes the need for a reformer system and uses an attractive fuel such as methanol, which has low price, and is easy to handle, store and transport<sup>4</sup>. However, it still needs further improvement to overcome several problems of methanol electro-oxidation reaction using platinum (Pt) catalyst, which is mostly used as the anode compartment in fuel cell. The catalytic activity of Pt is easily deactivated by poisoning effect from the methanol dehydrogenation process, which leads to reduced performance of the methanol electro-oxidation reaction<sup>5</sup>. This problem can be solved by modification of the second metal or using bimetallic electro-catalysts such as Ru, Sn, Mo, W and Os<sup>6</sup>. PtRu is considered to be the best available anodic material for DMFC<sup>7,8</sup>. This catalytic mechanism has been recognized by a bifunctional model and ligand or electronic effect model<sup>4,6,9</sup>. The binary PtRu catalyst can be prepared in various forms such as PtRu alloys, PtRu/C, Ru electrodeposited on Pt, PtRu co-deposited, and Ru adsorbed on Pt. The different PtRu preparations

exhibit the different electro-activities of the catalyst due to the dissimilarity in morphology, catalyst distribution and catalyst composition in electrode. Furthermore, the presence of high surface roughness of the electrode is one of the enhancement factors of methanol electro-oxidation reaction. The PtRu alloys can be easily prepared by chemical reduction process at room temperature, producing a very small and homogeneous particle. One of the reduction process is the Takenaka-Torikai method (T-T method), which gives high surface roughness by coating the reactive catalyst metals on the solid polymer electrolyte (SPE) membrane such as polyperfluorosulfonic acid membrane or Nafion<sup>®</sup> membrane<sup>3-5</sup>.

The purposes of this work were to study the electrochemical behavior of electro-oxidation reaction of methanol on Pt- and PtRu-SPE electrodes, in comparison with their micro- and nano-structure. The prepared electrodes were then characterized by scanning electron microscopy (SEM), electron dispersive X-ray microprobe (EDX), X-ray diffraction analysis and electrochemical techniques. The PtRu-SPE electrodes were prepared with a wide range of Ru:Pt ratio to examine the electro-oxidation efficiency of these catalyst, because the catalyst composition plays a functional role on the electro-catalytic behavior<sup>10-13</sup>. The T-T method, first reported by Takenaka and Co-worker<sup>14</sup>, was used to fabricate Pt

and PtRu alloy electrode on the SPE membrane.

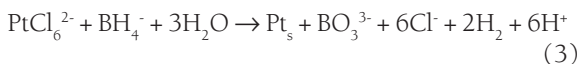
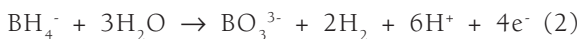
## MATERIALS AND METHODS

### Chemicals

All solutions were prepared with Milli-Q water system ( $18 \text{ M}\Omega \text{ cm}^{-1}$ ) and analytical grade chemicals: methanol (Merck),  $\text{H}_2\text{PtCl}_6 \cdot \text{H}_2\text{O}$  (Fluka),  $\text{RuCl}_3$  (Fluka),  $\text{NaBH}_4$  (Fluka), Nafion<sup>®</sup>-117 membrane (Fluka),  $\text{HNO}_3$  (Merck) and  $\text{H}_2\text{SO}_4$  (Merck).

### Methods for Electrodes Preparation

The Pt- and PtRu-Solid Polymer Electrodes (Pt-SPE and PtRu-SPE) were prepared by the modified Takenaka-Torikai (T-T) method<sup>15,16</sup>. In this method, the Nafion<sup>®</sup>-117 membrane was boiled in the solution of  $\text{HNO}_3\text{-H}_2\text{O}$  (1:1, v/v) for 1 hour and then in Milli-Q water for 1 hour. The SPE membrane was mounted on a vertical cell. The hexachloroplatinate ions ( $\text{PtCl}_6^{2-}$ ) and a reducing agent, tetrahydroborate ion ( $\text{BH}_4^-$ ), were exposed to the opposite site of a stationary solid polymer membrane. The  $\text{BH}_4^-$  ion can continuously penetrate into the membrane layer and come into contact with  $\text{PtCl}_6^{2-}$  ions on the opposite site of the membrane surface. The  $\text{PtCl}_6^{2-}$  ions were mostly reduced to form Pt metals on the membrane surface and partly deposited inside the membrane. The redox reaction<sup>14</sup> are shown in equation (1), (2) and (3) for the overall process.

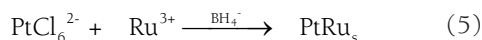


Then, the membrane electrode was soaked in 0.5 M  $\text{H}_2\text{SO}_4$  for 1 hour and kept in Milli-Q water prior to use. The obtained Pt electrode was designed as Pt-SPE. Variable parameters for Pt-SPE preparation were the concentration of  $\text{NaBH}_4$  and the deposition time. The optimum condition was considered from current density of methanol electro-oxidation reaction, Pt loading, and roughness factor (R).

The PtRu-SPEs were prepared in the same manner as described by introducing  $\text{RuCl}_3$  solution into  $\text{H}_2\text{PtCl}_6$  solution with different mole ratios as shown in Table 1. The  $\text{H}_2\text{PtCl}_6$  and  $\text{RuCl}_3$  solutions were exposed to the opposite sites of the  $\text{NaBH}_4$  solution on the SPE membrane. The reaction of PtRu catalyst preparation can be summarized in reaction (1), (2), and (4) for half-cell reactions of  $\text{PtCl}_6^{2-}$ ,  $\text{BH}_4^-$  and  $\text{Ru}^{3+}$ , respectively.



Therefore, the redox process can be explained by the overall reaction in equation (5).



### Electrochemical Studies

The electro-oxidation reaction of methanol is the major consideration for simplified study of the DMFC anode. The electrochemical characteristics of the electrodes were investigated by cyclic voltammetry (CV) and chronoamperometry using a standard three-electrode cell. The working electrode was the Pt- or PtRu-SPE, the counter electrode was a Pt rod, and the reference electrode was a Ag/AgCl electrode. All potentials are quoted against the Ag/AgCl reference electrode. A supporting electrolyte was 0.5 M  $\text{H}_2\text{SO}_4$  prepared in ultra pure water. All electrochemical experiments were carried out under nitrogen atmosphere and measured with the PGSTAT 30 AUTOLAB potentiostat/galvanostat system (Eco Chemie, Netherlands), which was controlled by GPES software. The SPEs were activated by cycling potential between  $-0.22$  and  $1.33 \text{ V}$  at scan rate of  $50 \text{ mVs}^{-2}$  until constant CV pattern was obtained.

The  $i(t)$ -E experiment plotted between current and electrode potential was used to determine the enhancement effect of adding Ru in the methanol electro-oxidation reaction. This plot was obtained from the chronoamperograms which were held at constant potentials of 0.3 and 0.4 V and collected the current at  $t = 200\text{s}$ . Cyclic voltammograms and chronoamperograms were obtained from the electro-oxidation of methanol experiments, which were carried out in a solution containing 0.5 M  $\text{H}_2\text{SO}_4$  and 0.1 M methanol at room temperature. These current densities were normalized to the geometrical electrode area for all experiments. The maximum peak current density ( $I_p$ ) was obtained from CV at ca. 0.6 V.

The roughness factor (R) is the ratio of the real active surface area ( $A_{\text{real}}$ ) to the geometrical surface area ( $A_{\text{geo}}$ ) of the Pt electrode<sup>17</sup>. The  $A_{\text{real}}$  was obtained from the ratio of the measurement of saturated hydrogen coverage ( $Q_{\text{H}}$ ) on electrode surface to the electrical charge associated with monolayer adsorption of hydrogen ( $Q_{\text{H,ref}} = 0.210 \text{ mCcm}^{-2}$ )<sup>18</sup> using CV technique, according to equations (6) and (7), respectively.

$$R = \frac{A_{\text{real}}}{A_{\text{geo}}} \quad (6)$$

$$A_{\text{real}} = \frac{Q_{\text{H}}}{Q_{\text{H,ref}}} \quad (7)$$

The results of R and  $I_p/R$  for Pt-SPE were compared with the electro-activity results from platinized Pt electrode (p-Pt) and smooth Pt electrode (s-Pt). The p-Pt is a modified electrode surface made by the electro-

deposition method for electro-activity enhancement.

## Morphology and Composition of the Electrodes

### Scanning electron microscope

The surface morphology of all membrane electrodes was examined by a JEOL, JMS-6400 scanning electron microscope (SEM). The line and area scans of elemental X-ray profile were obtained from an Oxford EDX Link, Series 300 Energy Dispersive X-ray spectrometer. The SPEs were cut and mounted on a carbon specimen SEM holder. Both surface and cross-section of SPE morphologies were investigated from the secondary electron micrograph at the appropriate magnification. The particle size distribution of accumulated Pt particle was calculated by KS 300K Ontron image analyzer software.

### X-ray diffraction

The Grazing incidence X-ray diffractometer used for analyzing the structures of electrodes was a Bruker D8 Advance diffractometer, with CuK $\alpha$  radiation. The X-ray source was operated at 40 kV and 40 mA. The measuring condition scans steps of 0.03° with a step time of 8 second. The small incidence angle ( $\alpha$ ) on specimen was set as 5°. The lattice parameters of Pt- and PtRu-SPEs were obtained from the fitting of Le Bail method by using Ritika program. The crystallite size of all electrodes was estimated from the broadening peak of the (220) reflection by using the Scherrer equation<sup>19</sup> and the Fundamental Parameter Approach (FPA) method<sup>20</sup>. The crystallite size or grain size distribution of catalyst was analyzed by Warren-Averbach method<sup>21</sup>.

### ICP-MS analysis

The Ru:Pt mole ratio of starting solution was calculated from the concentration of RuCl<sub>3</sub> and H<sub>4</sub>PtCl<sub>6</sub> solution and compared with the concentration values in the amount of adsorbed metal on SPE membrane, which were determined by ICP-MS (Perkin Elmer SCIEX model ELAN 6000). The samples of PtRu-SPE were dissolved in 20 ml of HCl:HNO<sub>3</sub> (2:1, v/v) solution for 15 hours. The samples were diluted 1000 times with 2% HNO<sub>3</sub> solution before being analysed by ICP-MS. Bi and Rh were used as internal standard. Calibration curves were constructed from the intensity of the analyte metal and concentration values. The Pt and Ru were detected at the signal of m/z 198 and 102, respectively.

## RESULTS AND DISCUSSION

### Characterization of Pt-SPE

The Pt catalyst was introduced on the Nafion®-117 surface by the modified T-T method. The effect of NaBH<sub>4</sub> concentration on the current density and the Pt loading,

at constant deposition time of 50 minutes is shown in Figure 1(a). The maximum current density was found at 0.095 M of NaBH<sub>4</sub> concentration, while the maximum Pt loading at 0.102 M of NaBH<sub>4</sub> concentration. For NaBH<sub>4</sub> concentration between 0.086 – 0.095 M, the increase in the current density was due to the increasing Pt loading on SPE membrane. The current density dropped when NaBH<sub>4</sub> concentration was higher than 0.095 M, and the Pt black particles were also observed in the solution. It is because BH<sub>4</sub><sup>-</sup> ions can rapidly penetrate across the membrane and then reacts with PtCl<sub>6</sub><sup>2-</sup> ions to form loosely packed Pt black particles on

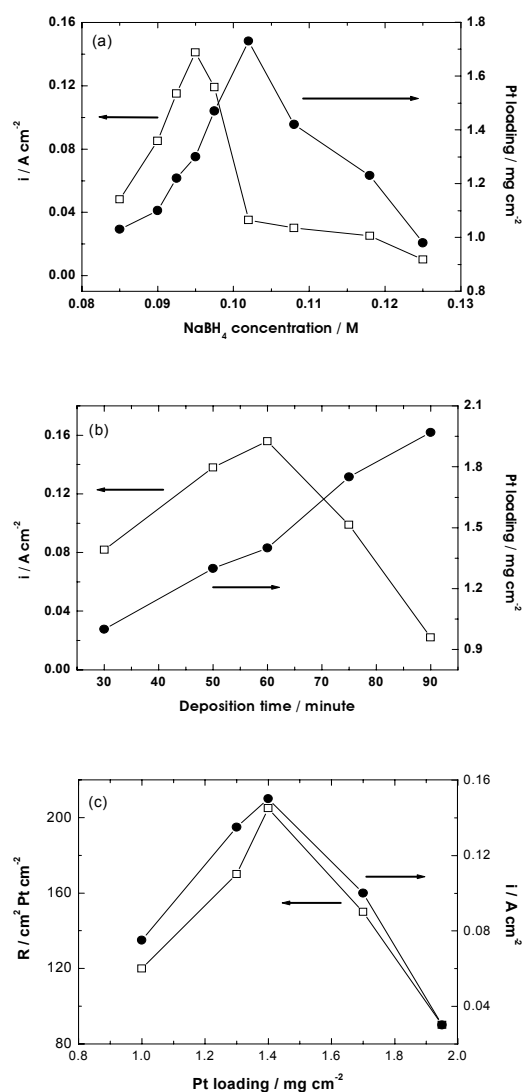


**Fig 1.** (a) The peak current density (□) and Pt loading (●) vs. the NaBH<sub>4</sub> concentrations at deposition time (50 minutes). (b) The peak current density (□) and Pt loading (●) vs. deposition time. (c) The roughness factor (□) and peak current density (●) vs. amount of Pt loading.

**Table 1.** The Ru:Pt ratio of Pt- and PtRu-SPE electrodes.

Electrodes	Concentration in starting solution			Metal concentration in PtRu-SPE electrodes		
	Pt/mM	Ru/mM	Ru:Pt mole ratio	Pt/mg cm <sup>-2</sup>	Ru/mg cm <sup>-2</sup>	Ru:Pt mole ratio
Pt	15.00	0.00	0.000	1.464	0.000	0.000
PtRu1	15.00	0.36	0.024	1.462	0.030	0.040
PtRu2	15.00	0.87	0.058	1.409	0.073	0.101
PtRu3	15.00	1.38	0.092	1.247	0.127	0.198
PtRu4	15.00	1.68	0.112	1.165	0.147	0.245
PtRu5	15.00	2.36	0.157	1.075	0.235	0.424
PtRu6	15.00	5.00	0.333	1.070	0.375	0.680
PtRu7	15.00	10.00	0.667	1.006	0.677	1.306

the opposite side of membrane. The 0.095 M was selected as the NaBH<sub>4</sub> concentration for all experiment.

The Figure 1(b) shows the effect of deposition time on the current density and Pt loading at 0.095M NaBH<sub>4</sub> concentration. The increasing deposition time gave higher Pt loading. However the maximum current density was found at the deposition time of 60 minutes and then the current density decreased with the increasing deposition time. According to Figure 1(a), the inactive Pt particles were found at long deposition time.

Figure 1(c) shows the relationship between electrode roughness factor (R) and the current density of methanol oxidation with increasing Pt loading. This result agrees well with Figure 1(a), indicating that the increase in an electro-activity is related to the roughness factor. Furthermore, at higher Pt loading, the Pt particles tended to be thicker and denser, which led to decreasing roughness factor.

The optimal condition for the Pt-SPE preparation was using 0.013 M PtCl<sub>6</sub><sup>2-</sup> solution and 0.095 M NaBH<sub>4</sub> solution with the deposition time of 60 minutes. The reproducibility for the electrochemical characteristic of Pt-SPE gave 0.156 ± 0.002 A/cm<sup>2</sup> (n = 3) for current density of methanol oxidation peak and 1.419 ± 0.041 mg/cm<sup>2</sup> (n = 3) for Pt loading.

The roughness factor and the peak current per roughness factor (I<sub>p</sub>/R) of Pt-SPE in the methanol electro-oxidation reaction were compared with those of p-Pt and s-Pt electrodes. The catalytic activity of Pt-SPE was significantly higher than the activity of p-Pt and s-Pt electrodes, which was indicated by the increasing I<sub>p</sub>/R values of the methanol oxidation peak. The I<sub>p</sub>/R value of Pt-SPE was greater than that p-Pt and s-Pt by 10.64 and 17.20 times, respectively. This might be due to high roughness factor of Pt-SPE and high surface area catalyst on the membrane electrodes.

### Characterization of PtRu-SPE

The PtRu-SPEs were prepared by the modified T-T method at various Ru contents. The notations of several

PtRu-SPEs are presented in Table 1. The ratios of Ru:Pt were calculated from the starting concentration of the H<sub>4</sub>PtCl<sub>6</sub> and RuCl<sub>3</sub> solutions and measured the metal on SPE electrode by ICP-MS with a good linear correlation of R<sup>2</sup> = 0.9923, as shown in the Table 1. The results of Ru:Pt also indicated that Ru<sup>3+</sup> ion may be easily reduced to metal than PtCl<sub>6</sub><sup>2-</sup> ion and it is possible that this catalyst preparation proceed via many processes.

The plot of electro-oxidation current against Ru:Pt ratios at 0.3 and 0.4 V is shown in Figure 2. The PtRu2-SPE (at Ru:Pt mole ratio = 0.10 or 10% Ru) presented the highest current for methanol electro-oxidation reaction at both observed potentials. This ratio can indicate that the electro-oxidation reaction of methanol proceed on Pt site more than Ru site. There were a number of published papers<sup>3, 8</sup>, which described the optimum condition of PtRu alloy for DMFC anode in the range of 10 – 40% Ru and 50% Ru for the oxidation of adsorbed CO<sub>ads</sub>.

The electrochemical oxidation of methanol on PtRu surface occurred in two steps as described by the bifunctional mechanism. The first step was methanol dehydrogenation in which methanol is oxidized to become adsorbed CO<sub>ads</sub> species. The second step was the removal of CO<sub>ads</sub> which proceeded via adsorbed OH<sub>ads</sub> to produce CO<sub>2</sub>. The adsorbed OH<sub>ads</sub> was produced from water dissociation process on both Pt and Ru catalyst sites. The overall processes are summarized in reaction (8), (9), and (10).



According to the above mechanism and several publications, methanol can be adsorbed and dissociated mainly on Pt while CO<sub>ads</sub> species can be adsorbed on both Pt and Ru. Therefore, the higher Pt content would be needed for methanol oxidation rather

than for  $\text{CO}_{\text{ads}}$  oxidation.

### Surface Characterization of Pt- and PtRu-SPE Electrodes

The three electrodes: Pt-SPE, PtRu2-SPE (the best electrode for methanol electro-oxidation reaction) and PtRu7-SPE (the highest Ru content) will be discussed. The SEM micrographs of Pt-SPE surface are shown in Figure 3. The low magnification SEM of the Pt-SPE surface morphology in Figure 3(a) shows the “micro cracks” in the platinum domain on Nafion<sup>®</sup> film. This cracking potentially occurred during the platinum formation process by internal tensile stress and lifetime limit of the electrode structure. The high-magnification micrograph in Figure 3(b) shows that the Pt-SPE has uniform spherical-like particles on the membrane surface. The surface of Pt was not made of smooth spherical particles as they were formed from many nano-spherical Pt particles as seen in Figures 3 (c and d).

The particle size distribution,  $g(D)$ , from SEM micrograph can be generally described by log-normal distribution function,<sup>22</sup> and can be directly calculated from Equation 11.

$$g(D) = \frac{1}{\sqrt{2\pi D \ln \sigma}} \exp \frac{-(\ln D - \ln \mu)^2}{2(\ln \sigma)^2} \quad (11)$$

where  $\mu$  is the most probable particle diameter, and  $\sigma$  is standard deviation for the distribution width.

The diameters of the Pt particles were in the range of 0.15 – 1.66  $\mu\text{m}$ , with the most probable particle diameter and standard derivation around 0.38 and 1.663  $\mu\text{m}$ , respectively. The particle sizes for PtRu2- and PtRu7-SPE were found at 0.44 and 0.57  $\mu\text{m}$ , respectively. The  $\sigma$  values for PtRu2- and PtRu7-SPE were 1.39 and 1.34  $\mu\text{m}$ , respectively. These results indicated that the particle size distribution of Pt- and PtRu-SPE was not significantly different. The little increase in particle size for PtRu catalyst might be caused by the existent of amorphous  $\text{RuO}_2$  or

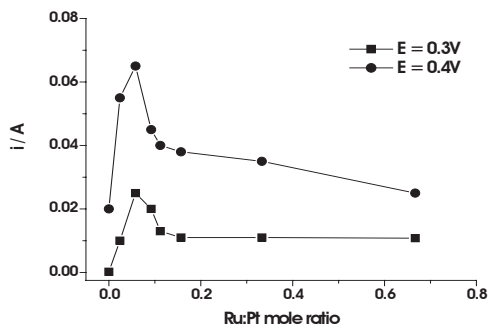
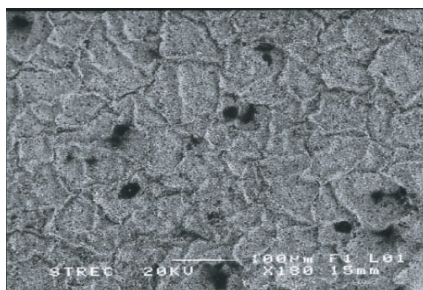


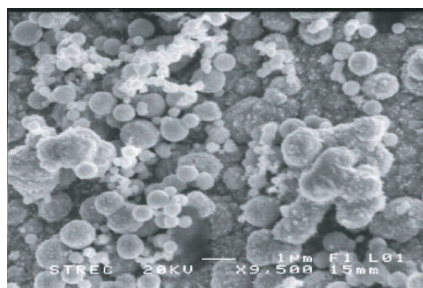
**Fig 2.** Relationship between methanol electro-oxidation current and Ru:Pt ratio at 0.3 and 0.4 V ( $t = 200\text{s}$ ) for PtRu-SPE electrodes.

amorphous  $\text{Ru}^3$ .

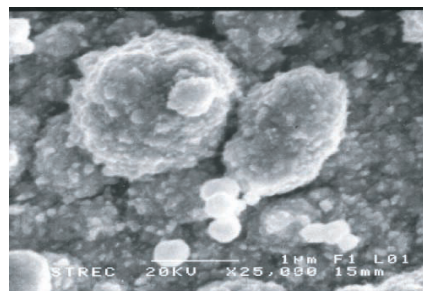
The EDX line scan in the cross section of Pt-SPE is shown in Figure 4. This line is demonstrated by a white line on the SEM micrograph in Figure 4(a). The EDX line scan profiles recorded the characteristic peaks of Pt



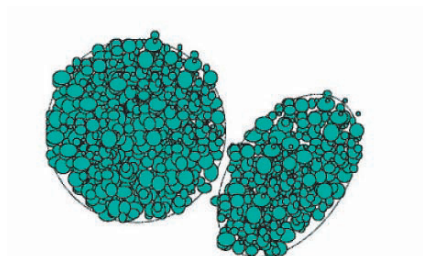
(a)



(b)



(c)



(d)

**Fig 3.** The SEM micrographs of Pt-SPE electrode; (a) x180, (b) x9500 and (c) x25000 magnification (d) schematic representation of the accumulating Pt particle.

M-line (solid line) and fluoride K-line (dash line) shown in Figure 4(b). The EDX profile of fluoride can be used as a marker for indicating the membrane edge at the relative length of 20 mm from the starting point. The profile of Pt started at 14 mm and increased rapidly at the membrane edge of 20 mm. The overlap of the dotted and solid lines between 14-22 mm indicated that Pt particles could penetrate about 5-6 mm into the SPE membrane. The Pt-line profile from 20 mm to 32 mm confirmed that Pt was mainly introduced onto the membrane surface with approximately 12 mm thickness.

The cross-section of SEM micrographs for PtRu2 and PtRu7-SPE electrodes are shown in Figures 4 (c and d). These results found that the metal layer

penetrated about 3-6  $\mu\text{m}$  into the membrane and the thicknesses were ca. 10  $\mu\text{m}$ . No EDX line scan of Ru element in PtRu2-SPE electrode was possible because the concentration of Ru is lower than the instrumental detection limit. However, the EDX line scan profile of PtRu7-SPE electrode showed that the Ru element was homogeneously distributed on the metal layer, which could be observed from the overlap of EDX line scan of both Pt and Ru.

The metal distributions of Pt or Ru elements on the electrode surface are shown in Figure 5. These results showed good distribution of Pt on the surface of both electrodes. The Ru signal from PtRu2-SPE found the metal distribution on the electrode surface. However, the Ru EDX area scan result of PtRu7-SPE clearly

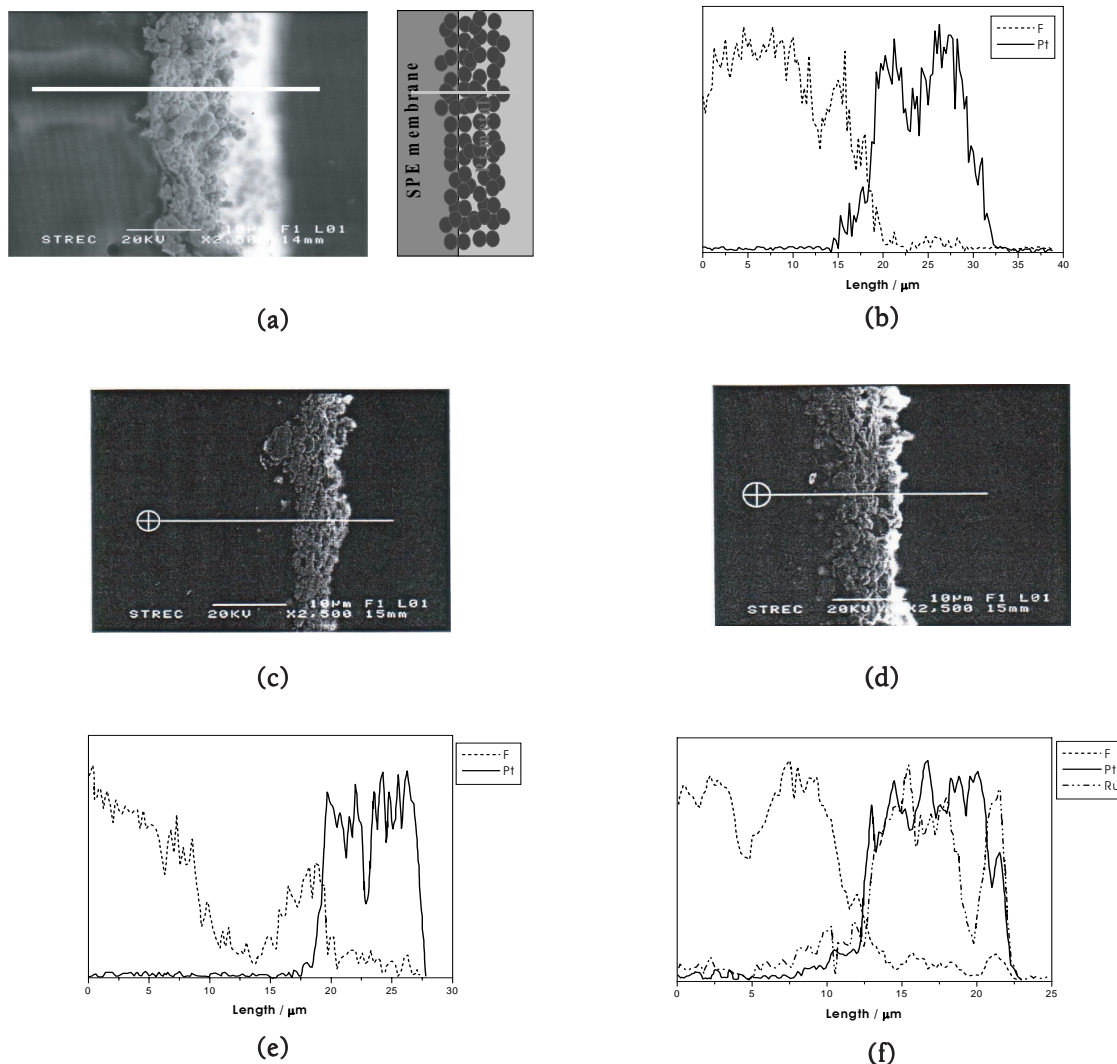


**Fig 4.** (a) The morphology of Pt-SPE electrode, (b) The cross-section EDX line scan of Pt-SPE electrode, (c) The morphology of PtRu2-SPE electrode, (d) The morphology of PtRu7-SPE electrode, (e) The cross-section EDX line scan of PtRu2-SPE and (f) The cross-section EDX line scan of PtRu7-SPE.

demonstrated the agglomeration of Ru element on the electrode surface, indicating the immiscibility of Ru element with the Ru-rich condition.

X-ray diffraction (XRD) patterns of three electrodes are shown in Figure 6(a). This peak pattern of Pt-SPE electrode indicated a face-centered cubic (fcc) structure. PtRu-SPE displayed the diffraction patterns similar to those of the Pt-SPE, except for the shift of  $2\theta$  values to slightly higher values and the increase in peak broadening with increasing Ru content, indicating a decrease of both lattice parameter and crystallite size <sup>20-21</sup>.

The phase diagram<sup>23</sup> of Pt-Ru showed that Pt and Ru metal generated the solid solution when Ru content was less than 62%, forming a fcc Pt structure. However, when Ru content was greater than 62%, the two phase region of the fcc Pt and the hexagonal closest packed (hcp) Ru structure was observed. In this experiment, the XRD results of all electrodes showed only the fcc Pt structure. It is suggested that Pt and Ru in PtRu catalysts formed a solid solution in a mixture of both metals. Pt atoms were replaced by Ru atoms in fcc structure. However, hcp structure of Ru phase could

**Table 2.** Variation of average crystallite size with increasing Ru content.

Samples	Ru:Pt mole ratio	Line broadening peak method		FPA /nm
		Peason VI/nm	Pseudo-Voigt/nm	
Pt	0.000	11.5	12.3	12.2
PtRu1-SPE	0.040	10.4	11.4	11.4
PtRu2-SPE	0.101	9.8	10.4	10.1
PtRu3-SPE	0.198	8.5	9.0	9.0
PtRu4-SPE	0.245	8.8	9.3	9.8
PtRu5-SPE	0.424	8.0	8.1	8.0
PtRu6-SPE	0.680	6.0	6.1	6.1
PtRu7-SPE	1.306	6.1	6.3	6.6

not be found in PtRu7 (Ru-rich condition). It is possible that the increasing Ru content could result in an amorphous RuO<sub>2</sub> or Ru phase<sup>3</sup>.

Furthermore, the formation of PtRu alloy could be explained in the term of the decreasing lattice parameter ( $a_{fcc}$ ). This phenomenon is called the Vegard's law<sup>24</sup>. The crystallographic data is shown in Table 2. The lattice parameter progressively decreased for the PtRu with respect to the increasing Ru content in PtRu-SPE. However, the lattice parameters did not significantly change in PtRu6- and PtRu7-SPEs. It can confirm that the formation of amorphous RuO<sub>2</sub> could be found, according to the former discussion. The crystallite size distribution of Pt- and PtRu-SPE is shown in Figure 6(b). The distribution function has significantly

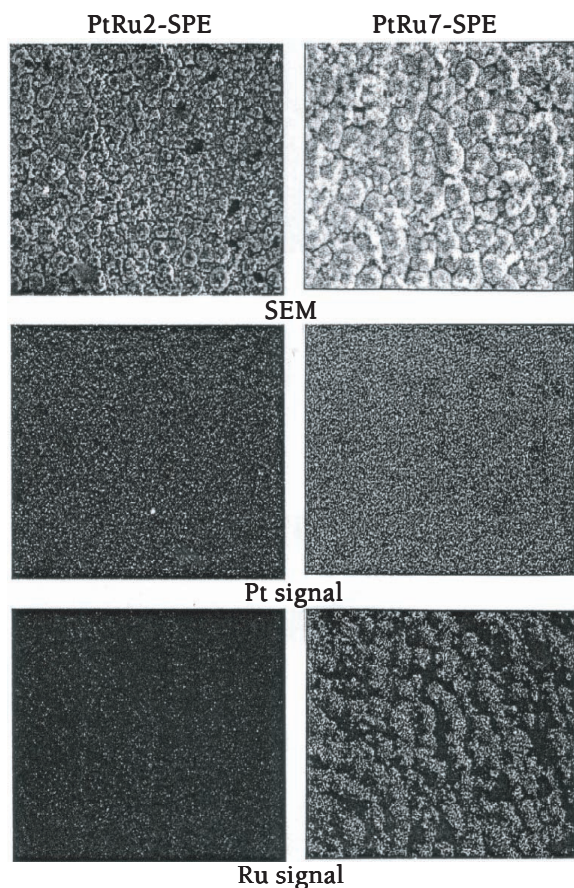


**Fig 5.** The EDX area scan profiles of Pt and Ru of PtRu2- and PtRu7-SPE electrodes.

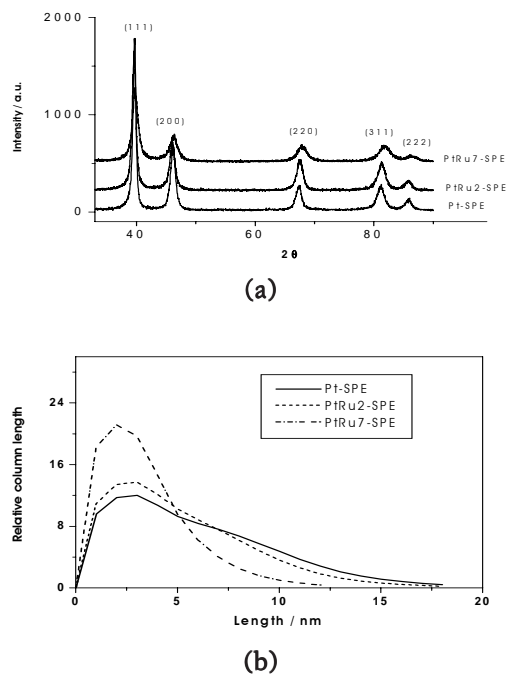


**Fig 6.** (a) XRD patterns and (b) a log-normal distribution of crystallite size of Pt-, PtRu2- and PtRu7-SPE electrodes.

narrowed down with the increasing Ru contents, which agreed very well with the results of Vegard's law.

## CONCLUSION

The Pt- and PtRu-SPEs, which were prepared by the modified T-T method showed the high surface roughness and formation of agglomerate nanoparticles. The best electrode for the methanol electro-oxidation reaction is PtRu<sub>2</sub>-SPE with the mole ratio of 0.10. The CV results also confirmed the presence of high roughness factor for the obtained electrodes. XRD results confirmed the formation of nano-sized catalyst and the PtRu alloy with the fcc Pt structure. The increasing Ru content led to the decrease in lattice parameters and size distribution due to Pt-Ru solid solution phenomena. However, the Ru-rich condition brought the formation of amorphous Ru or RuO<sub>2</sub> on the electrode surface. These studies present the promising PtRu-SPE for use in methanol fuel cell as it gains high electro-activity of methanol oxidation reaction.

## ACKNOWLEDGEMENTS

This work was financially supported by the research grant from Master Degree Research Fund under the Energy Conservation Promotion Fund, National Energy Policy Office, and from Postgraduate Education and Research in Chemistry (PERCH).

## REFERENCES

- Zhou WJ et al. (2004) Performance comparison of low-temperature direct alcohol fuel cells with different anode catalysts. *J. Power Sources* **126**, 16-22.
- Hoogers G (2003) Fuel cell technology handbook, CRC Press.
- Cameron, D.S. (2003) Fuel cells-science and technology 2002. *Platinum Metals Rev.* **47** (1), 28-31.
- Zerbinati O, Mardan A and Richter MM (2002) A direct methanol fuel cell. *J. Chem. Educ.* **79** (7), 829-31.
- Vigier F, Coutanceau C, Perrard A, Belgsir EM and Lamy C (2004) Development of anode catalysts for a direct ethanol fuel cell. *J. Appl. Electrochem.* **34**, 439-46.
- Antolini E (2003) Formation of carbon-supported PtM alloys for low temperature fuel cell: a review. *Mat. Chem. Phys.* **78**, 563-73.
- Dinh HN, Ren X, Garzon FH, Zelenay P and Gottesfeld S (2000) Electrocatalysis in direct methanol fuel cells: in-situ probing of PtRu anode catalyst surfaces. *J. Electroanal. Chem.* **491**, 222-33.
- Iwasita T, Hoster H, John-Anacker A, Lin WF and Vielstich W (2000) Methanol oxidation on PtRu electrodes. Influence of surface structure and Pt-Ru atom distribution. *Langmuir* **16**, 522-9.
- Gellings PJ and Bouwmeester HJM (1997) The CRC handbook of solid state electrochemistry, CRC Press.
- Seiler T, Savinova ER, Friedrich KA and Stimming U (2004) Poisoning of PtRu/C catalysts in the anode of a direct methanol fuel cell: a DEMS study. *Electrochim. Acta* **49**, 3927-36.
- Waszczuk P, Lu GQ, Wieckowski A, Lu C, Rice C and Masel RI (2002) UHV and electrochemical studies of CO and methanol adsorbed at platinum/ruthenium surface, and reference to fuel cell catalysis. *Electrochim. Acta* **47**, 3637-52.
- Tong YY, Kim HS, Babu PK, Waszczuk P, Wieckowski A and Oldfield E (2002) An NMR investigation of CO tolerance in a Pt/Ru fuel cell catalyst. *J. Am. Chem. Soc.* **124** (3), 468-73.
- Kabbabi A et al. (1998) In situ FTIR study of the electrocatalytic oxidation of carbon monoxide and methanol at platinum-ruthenium bulk alloy electrodes. *J. Electroanal. Chem.* **444**, 41-53.
- Sheppard SA, Campbell SA, Smith JR, Lloyd GW, Ralph TR and Walsh FC (1998) Electrochemical and microscopic characterisation of platinum-coated perfluorosulfonic acid (Nafion 117) materials. *Analyst* **123**, 1923-9.
- Aramata A and Ohnishi R (1984) Methanol electrooxidation on platinum directly bonded to a solid polymer electrolyte membrane. *J. Electroanal. Chem.* **162**, 153-62.
- Aramata A and Masuda M (1991) Platinum alloy electrodes bonded to solid polymer electrolyte for enhancement of methanol electro-oxidation and its reaction mechanism. *J. Electrochem. Soc.* **138** (7), 1949-57.
- Rodriguez JMD, Melian JAH and Pena JP (2000) Determination of the real surface area of Pt electrodes by hydrogen adsorption using cyclic voltammetry. *J. Chem. Educ.* **77** (9), 1195-7.
- Manoharan R and Prabhuram J (2001) Possibilities of prevention of formation of poisoning species on direct methanol fuel cell anodes. *J. Power Sources* **96**, 220-5.
- Antolini E, Giorgi L, Cardellini F and Passalacqua E (2001) Physical and morphological characteristics and electrochemical behavior in PEM fuel cells of PtRu/C catalysts. *J. Solid State Electrochem.* **5** (2), 131-40.
- Ortiz AL, Cumbre FL, Sanchez-Baja F, Guiberteau F and Caruso R (2000) Fundamental parameters approach in the Rietveld method: a study of the stability of results results the accuracy of the instrumental. *J. European Cee. Soc.* **20**, 1845-51.
- Guerrero-Paz J and Jaramillo-Vigueras D (1999) Comparison of grain size distribution obtained by XRD and TEM in milled FCC powders. *NanoStructure Materials* **11** (8), 1195-204.
- Granqvist CG and Buhrman RA (1976) Ultrafine metal particles. *J. Appl. Phys.* **47** (5), 2200-19.
- Richarz F, Wohlmann B, Vogel U, Hoffschulz H and Wlaus W (1995) Surface and electrochemical characterization of electrodeposited PtRu alloys. *Surface Science* **335**, 361-71.
- Loffler MS, Natter H, Hempelmann R and Wippermann K (2003) Preparation and characterisation of Pt-Ru model electrodes for the direct methanol fuel cell. *Electrochim. Acta* **48**, 3047-51.